JOURNAL OF CHEMICAL PHYSICS VOLUME 109, NUMBER 2 8 JULY 1998

Singularity-free interpretation of the thermodynamics of supercooled water. II. Thermal and volumetric behavior

Luis Paulo N. Rebelo,[a] Pablo G. Debenedetti,[b] and Srikanth Sastry[c]
Department of Chemical Engineering, Princeton University, Princeton, New Jersey 08544-5263

(Received 23 February 1998; accepted 3 April 1998)

According to the singularity-free interpretation of the thermodynamics of supercooled water, the isothermal compressibility, isobaric heat capacity, and the magnitude of the thermal expansion coefficient increase sharply upon supercooling, but remain finite. No phase transition or critical point occurs at low temperatures. Instead, there is a pronounced but continuous increase in volume and a corresponding decrease in entropy at low temperatures, the sharpness of which becomes more pronounced the lower the temperature and the higher the pressure. We investigate the behavior of the response functions, equation of state, and entropy of a schematic waterlike model that exhibits singularity-free behavior, and thereby illustrate the simplest thermodynamically consistent interpretation that is in accord with existing experimental evidence on water's low-temperature anomalies. In spite of its simplicity, the model captures many nontrivial aspects of water's thermodynamics semiquantitatively. © *1998 American Institute of Physics.* [S0021-9606(98)51626-1]

I. INTRODUCTION

Understanding the phase behavior of metastable water at low temperatures remains one of the most interesting and important open questions in the physical sciences.[1–3] Although more than a quarter century has elapsed since anomalous increases in the response functions of liquid water upon supercooling were first reported,[4,5] a clear understanding of the underlying phase behavior remains elusive. Three thermodynamically consistent interpretations have been proposed to explain the experimental observations. The stability limit conjecture[6–8] posits the existence of a retracing spinodal curve bounding the superheated, stretched, and supercooled states of metastable water, and attributes the anomalous increases in the response functions to proximity to the spinodal curve. The two critical point hypothesis[9–16] posits the existence of a line of first-order transitions between two distinct forms of liquid water, terminating at a metastable critical point. The anomalous increase in the response functions is here attributed to the presence of this critical point. In the singularity-free scenario the response functions remain finite, and exhibit extrema but no divergences.[17,18] Thus, the response functions are predicted to diverge in the former two scenarios, but remain finite in the latter.

Because of the difficulties associated with making measurements on a highly metastable liquid at extreme conditions of temperature and pressure,[19,20] the available experimental evidence is inconclusive, and none of the three scenarios mentioned before has been unambiguously proved or disproved. Evidence in support of the two critical point hypothesis includes thermal and volumetric measurements on glassy water that are not inconsistent with the existence of a first-order transition between two distinct forms,[19–22] computer simulations,[9,11,14,15] and theoretical calculations.[12,13] Low-temperature extrapolations of numerous equilibrium and transport properties are not inconsistent with the stability-limit conjecture.[1–3,5] Low-angle x-ray scattering experiments[23] and theoretical calculations,[17,18] on the other hand, support the singularity-free scenario.

In a recent paper,[18] we proposed and examined the singularity-free scenario. Specifically, we showed that the increase in the isothermal compressibility upon supercooling is inseparable from the existence of a negatively sloped locus of density maxima, such as water possesses over a broad range of pressures and temperatures.[24] Furthermore, we showed that large increases in compressibility can occur in the absence of any assumed low-temperature singularity, be it a spinodal curve or a critical point. Thus, from purely thermodynamic arguments, we showed that the simplest interpretation of the experimental observations on the behavior of supercooled water is devoid of singularities. In that work we also proposed a simple compressible lattice model in which molecules can form directional bonds, and which displayed singularity-free behavior. We used the model to illustrate the simplest volumetric (P,v,T) behavior that can explain water's low-temperature anomalies. Although we solve the lattice model in the mean-field approximation, the absence of a second critical point is a feature of the model, and not an artifact of the solution technique.[18]

Here, we extend our previous work by studying the model's entropy, as well as its volumetric behavior, over wide ranges of temperature and pressure. Whereas in the previous paper we studied the isothermal compressibility, here we

---

[a] Permanent address: Departamento Quimica, Faculdade de Ciencias e Tecnologia, Universidade Nova de Lisboa, 2825 Monte da Caparica, Lisbon, Portugal.

[b] Author to whom correspondence should be addressed. Electronic mail: pdebene@pucc.princeton.edu

[c] Permanent address: Jawaharlal Nehru Center for Advanced Scientific Research, Bangalore 560064, India. Electronic mail: sastry@jncasr.ac.in

also investigate the temperature and pressure dependence of the isobaric heat capacity and the thermal expansion coefficient. We provide here, therefore, a thorough investigation of the thermal and volumetric implications of the singularity-free scenario. We use the idealized model descriptively, not predictively. By this we mean that the simplifications built into the model's formulation preclude its predictive use. Although the model captures, semiquantitatively, many nontrivial aspects of water's thermodynamics, our primary interest is not in this numerical agreement, but in understanding the overall topological features of a thermal and volumetric equation of state that is consistent with the experimentally observed anomalous behavior upon supercooling, yet does not require underlying singularities to produce the anomalies.

The paper is structured as follows. In Sec. II we present thermodynamic relations that provide consistency checks for the model calculations. In Sec. III we summarize the microscopic model and present new expressions for the response functions and for the entropy. In Sec. IV we present the calculations on the model's thermal and volumetric behavior over a wide range of temperatures and pressures. Finally, in Sec. V we summarize the main conclusions that follow from the calculations, and discuss their consequences for future experiments on supercooled and glassy water.

II. THERMODYNAMIC ANALYSIS

We first consider the relationship between the pressure dependence of the thermal expansion coefficient α_p, and the temperature dependence of the isothermal compressibility K_T,

$$\alpha_p=\frac{1}{v}\left(\frac{\partial v}{\partial T}\right)_P, \quad K_T=-\frac{1}{v}\left(\frac{\partial v}{\partial P}\right)_T$$

where v is the molar volume. To this end, we start from the thermodynamic relations

$$v\alpha_p=\frac{\partial^2 g}{\partial T\partial P}, \quad vK_T=-\frac{\partial^2 g}{\partial P^2}, \tag{1}$$

where g is the molar Gibbs energy. One then has

$$\left(\frac{\partial v\alpha_p}{\partial P}\right)_T=-\left(\frac{\partial vK_T}{\partial T}\right)_P=\frac{\partial^3 g}{\partial P^2\partial T} \tag{2}$$

and, therefore,

$$\left(\frac{\partial \alpha_p}{\partial P}\right)_T=-\left(\frac{\partial K_T}{\partial T}\right)_P. \tag{3}$$

Equation (3) shows that the locus of temperature extrema of K_T along isobars coincides with the locus of pressure extrema of α_p along isotherms.[25]

In Ref. 18 we derived the following identity:

$$\left(\frac{\partial K_T}{\partial T}\right)_{P,\ \text{at TMD}}=\frac{1}{v}\frac{(\partial^2 v/\partial T^2)_{P,\text{at TMD}}}{(dP/dT)_{\text{TMD}}}, \tag{4}$$

where TMD denotes the locus of density maxima (or temperature of maximum density), in the (P,T) plane; the subscript ''at TMD'' signifies that the partial derivative is evaluated at a point belonging to the TMD locus; and the subscript TMD signifies that the derivative is evaluated along the direction of the TMD locus, at the state point of interest. The numerator on the right-hand side of Eq. (4) is necessarily positive at the TMD.[18] Since Eq. (3) is also valid at any point along the TMD, it follows that

$$\left(\frac{\partial \alpha_p}{\partial P}\right)_{T,\text{at TMD}}=-\frac{1}{v}\frac{(\partial^2 v/\partial T^2)_{P,\text{at TMD}}}{(dP/dT)_{\text{TMD}}}. \tag{5}$$

Equation (5) shows that when the TMD has a negative slope, α_p decreases upon isothermal decompression. Since in that case α_p is negative below the TMD (i.e., for $P<P_{\text{TMD}}$ at the given T), this means that the magnitude of α_p increases upon isothermal decompression in the vicinity of the TMD. Conversely, when the TMD has positive slope, in which case the thermal expansion coefficient is negative above the TMD, α_p increases upon isothermal decompression. Thus, if the TMD retraces in the (P,T) plane, the magnitude of α_p exhibits a maximum (α_p exhibits a minimum) with respect to pressure at constant temperature, for all temperatures lower than the ''nose'' of the TMD, where dP/dT diverges.

Proceeding as in Eqs. (1)–(3), one has the identities

$$-\frac{1}{T}\left(\frac{\partial c_p}{\partial P}\right)_T=\left(\frac{\partial^2 v}{\partial T^2}\right)_P=\frac{\partial^3 g}{\partial T^2\partial P}, \tag{6}$$

where c_p is the isobaric heat capacity,

$$c_p=T\left(\frac{\partial s}{\partial T}\right)_P$$

with s, the molar entropy. Equations (3)–(6) will be used to interpret the thermal and volumetric behavior described in Sec. IV.

III. MODEL

In Ref. 18 a microscopic waterlike model was formulated and its equation of state was derived. This equation of state displayed many nontrivial features characteristic of water. These include negative thermal expansion, and a marked increase of the isothermal compressibility upon supercooling. In addition, the behavior of the compressibility upon supercooling was found to conform with the singularity-free scenario for the global phase behavior of supercooled water. By this is meant behavior that is consistent with experimental observations and according to which the observed increases in the response functions of supercooled water at low temperatures[4,5,26,27] occur in the absence of a retracing spinodal curve bounding the supercooled and stretched states of metastable water,[6] and in the absence, too, of a metastable critical point.[16] This is significant because thermodynamics imposes constraints on the possible types of thermal and volumetric behavior that are consistent with increases in compressibility, isobaric heat capacity, and in the magnitude of the (negative) thermal expansion coefficient upon isobaric cooling.[7,8] Thus, it has only been possible to propose a small number of thermodynamically consistent scenarios to explain the observed thermal and volumetric properties of supercooled water. The singularity-free scenario is one of them, the other two being the retracing spinodal conjecture of Speedy[6] and the two-critical point hypothesis of Poole *et al.*[9]

In Ref. 18, only a few features of the singularity-free scenario were investigated. In particular, only the behavior of the compressibility, but not that of the isobaric heat capacity or the thermal expansion coefficient, were addressed. The system's volume, but not its entropy, was studied. Here, we extend our initial analysis by studying the entropy, equation of state, isobaric heat capacity, and thermal expansion coefficient. The model is a lattice fluid in which pairs of molecules, in addition to interacting through the usual hard-core (single-occupancy) and van der Waals (nearest-neighbor attraction) forces, can form hydrogen bonds if correctly oriented. Furthermore, in order to incorporate the correlation between local density and bonding energy that is a distinguishing feature of water (that is to say, the fact that regions with strong hydrogen bond interactions have lower density, energy, and entropy than regions with weaker bonded interactions), the volume associated with a pair of sites is greater if these sites are occupied by a bonded pair than either if the pair is not bonded, or if one or both sites are unoccupied. In other words, the model uses the lattice geometry simply as a reference topology for defining interacting neighbors, and calls for the calculation of the system's volume as the expectation value of the volumes associated with pairs of neighboring sites. A detailed derivation of the equation of state is given in Ref. 18, and will not be repeated here. We merely mention that the fact that the system's volume is not fixed requires that the model be formulated in the generalized ensemble, whose independent variables are (P, μ, and T), and the relevant thermodynamic potential for which, $U-TS+PV-\mu N$, is identically 0. The equation of state was obtained by solving the model in the mean-field approximation. The chemical potential and equation of state are given by

$$\mu=-\gamma kT\ \ln q-2\tilde{\epsilon}n+kT\ \ln\left(\frac{n}{1-n}\right), \tag{7}$$

$$P\nu_0=-\tilde{\epsilon}n^2-kT\ \ln(1-n), \tag{8}$$

where γ is the coordination number, q is the number of distinguishable orientations of a given molecule with respect to a given nearest neighbor, n is the fraction of sites that is occupied, and

$$\tilde{\epsilon}=\gamma(\epsilon+\delta J_p)/2, \tag{9}$$

$$\delta J_p=kT\ \ln\left[1+q^{-1}(e^{J_p/kT}-1)\right], \tag{10}$$

$$J_p=J-P\,\delta b. \tag{11}$$

In the above equations, ϵ is the van der Waals interaction strength between two occupied nearest-neighbor (nn) sites; J is the hydrogen-bonded interaction strength between two correctly oriented nn molecules, and the system's volume is given by

$$V=\sum_{\langle i,j\rangle} b_{ij}, \tag{12}$$

where $\langle i,j\rangle$ denotes summation of nn pairs, and the volume associated with each pair is given by

$$b_{ij}=\begin{cases} b & \text{NHB or } (n_i \text{ or } n_j=0) \\ b+\delta b & \text{HB.} \end{cases} \tag{13}$$

In Eq. (13), HB denotes a hydrogen-bonded pair, $n_i=1$ if site i is occupied, and 0 if it is empty, and NHB denotes a non-hydrogen-bonded pair. The relationship between b and ν_0 is given by $\nu_0=\gamma b/2$. The specific volume follows from differentiating the chemical potential,

$$\nu=\left(\frac{\partial\mu}{\partial P}\right)_T=-2n\left(\frac{\partial\tilde{\epsilon}}{\partial P}\right)_T+\left(-2\tilde{\epsilon}+\frac{kT}{n-n^2}\right)\left(\frac{\partial n}{\partial P}\right)_T \tag{14}$$

and the pressure dependence of the fractional occupancy is obtained from the equation of state,

$$\left(\frac{\partial n}{\partial P}\right)_T=\frac{\nu_0+\left(\frac{\partial\tilde{\epsilon}}{\partial P}\right)_T n^2}{\frac{kT}{1-n}-2\tilde{\epsilon}n}. \tag{15}$$

It follows from Eqs. (14) and (15) that

$$\nu=\frac{\nu_0}{n}-n\left(\frac{\partial\tilde{\epsilon}}{\partial P}\right)_T=\frac{\nu_0}{n}+n\ \frac{\gamma\delta b}{2q}\ \exp[(J_p-\delta J_p)/kT], \tag{16}$$

where use has been made of Eqs. (9)–(11) to evaluate the pressure dependence of $\tilde{\epsilon}$. In summary, the (P,ν,T) equation of state is given by Eqs. (8) and (16), with the various quantities defined as in Eqs. (9)–(11). For any given (P,T), n is obtained from Eq. (8) and ν from Eq. (16). The model's entropy is given by

$$\begin{aligned} s&=-\left(\frac{\partial\mu}{\partial T}\right)_P \\ &=\gamma k\ \ln q+2n\left(\frac{\partial\tilde{\epsilon}}{\partial T}\right)_P-k\ \ln\left(\frac{n}{1-n}\right) \\ &\quad+\left[2\tilde{\epsilon}-kT\left(\frac{1}{n}+\frac{1}{1-n}\right)\right]\left(\frac{\partial n}{\partial T}\right)_P. \end{aligned} \tag{17}$$

Again, dn/dT follows from Eq. (8),

$$\left(\frac{\partial n}{\partial T}\right)_P=-\frac{k\ \ln(1-n)+(\partial\tilde{\epsilon}/\partial T)_P n^2}{\frac{kT}{n-1}+2\tilde{\epsilon}n}, \tag{18}$$

whereupon the entropy per molecule becomes

$$\begin{aligned} s/k&=\gamma\ \ln q-\frac{1}{n}\ln(1-n)+\ln\left(\frac{1-n}{n}\right) \\ &\quad+\frac{\gamma n}{2kT}\{\delta J_p-q^{-1}J_p\ \exp[(J_p-\delta J_p)/kT]\}. \end{aligned} \tag{19}$$

Finally, the response functions are obtained as follows:

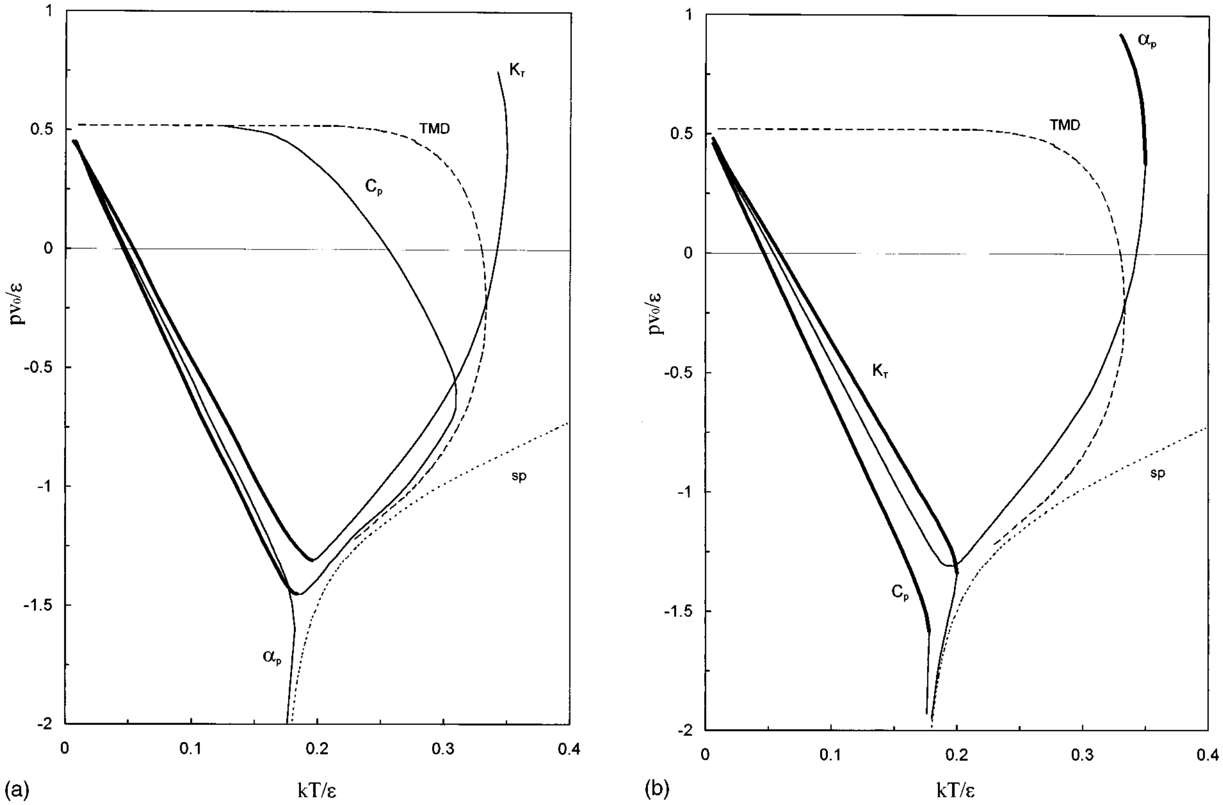

FIG. 1. General behavior predicted by the compressible lattice model. $\delta b/b=0.953$, $J/\epsilon=0.25$, $q=100$, $\gamma=4$. TMD is the locus of density maxima, sp is the spinodal for the superheated liquid. The lines labeled α_p, c_p, and K_T are extrema loci for the respective response functions, with thin lines denoting minima, and thick lines denoting maxima. In (a) the extrema are with respect to temperature (i.e., the figure must be ''read'' along isobars). In (b) the extrema are with respect to pressure (the figure must be ''read'' along isotherms).

$$c_p=T\left(\frac{\partial s}{\partial T}\right)_P=nT\left(\frac{\partial^2\tilde{\epsilon}}{\partial T^2}\right)_P+T\left(\frac{\partial n}{\partial T}\right)_P\left[\left(\frac{\partial\tilde{\epsilon}}{\partial T}\right)_P+\frac{k}{n^2}\ln(1-n)\right], \tag{20}$$

$$\alpha_p=\frac{1}{v}\left(\frac{\partial v}{\partial T}\right)_P=-\frac{1}{v}\left\{\left(\frac{\partial n}{\partial T}\right)_P\left[\frac{v_0}{n^2}+\left(\frac{\partial\tilde{\epsilon}}{\partial P}\right)_T\right]+n\,\frac{\partial^2\tilde{\epsilon}}{\partial T\partial P}\right\}, \tag{21}$$

$$K_T=-\frac{1}{v}\left(\frac{\partial v}{\partial P}\right)_T=\frac{1}{v}\left\{\left(\frac{\partial n}{\partial P}\right)_T\left[\frac{v_0}{n^2}+\left(\frac{\partial\tilde{\epsilon}}{\partial P}\right)_T\right]+n\,\frac{\partial^2\tilde{\epsilon}}{\partial P^2}\right\}, \tag{22}$$

where the temperature and pressure first derivatives of $\tilde{\epsilon}$ and n are obtained from Eqs. (9) to (11), and the second derivatives of $\tilde{\epsilon}$ also follow from Eqs. (9) to (11), and are given below,

$$\left(\frac{\partial^2\tilde{\epsilon}}{\partial P^2}\right)_T=\frac{\gamma(\delta b)^2}{2qkT}\exp[(J_p-\delta J_p)/kT]\times\{1-q^{-1}\exp[(J_p-\delta J_p)/kT]\}, \tag{23}$$

$$\left(\frac{\partial^2\tilde{\epsilon}}{\partial T^2}\right)_P=\frac{\gamma J_p}{2qT^2}\frac{J_p}{kT}\exp[(J_p-\delta J_p)/kT]\times\{1-q^{-1}\exp[(J_p-\delta J_p)/kT]\}, \tag{24}$$

$$\frac{\partial^2\tilde{\epsilon}}{\partial T\partial P}=\frac{\gamma\delta b}{2qT}\frac{J_p}{kT}\exp[(J_p-\delta J_p)/kT]\times\{1-q^{-1}\exp[(J_p-\delta J_p)/kT]\}. \tag{25}$$

IV. RESULTS AND DISCUSSION

Figure 1 shows the general behavior predicted by the model. In Fig. 1(a) are shown the TMD locus, the spinodal curve for the superheated liquid, and the locus of extrema of the isothermal compressibility, isobaric heat capacity, and thermal expansion coefficient. The distinguishing feature is the retracing TMD locus. The existence of this feature in water was first proposed by Poole and co-workers.[9]

The extrema in Fig. 1(a) are with respect to temperature, which means that this figure must be ''read'' along isobars. The locus of compressibility and heat capacity extrema includes minima (thin lines) and maxima (thick lines). The locus of α_p extrema gives the pressure-dependent temperature at which the negative thermal expansion reaches a minimum (absolute value reaches a maximum). Another salient feature of Fig. 1(a) is the fact that the three response functions show low-temperature extrema with respect to temperature, the loci of which are very close to each other. Physically, this corresponds to a marked increase in the magnitude of the three response functions upon isobaric supercooling. In agreement with the experimental behavior of water, one finds along isobars a pair of compressibility and heat capac-

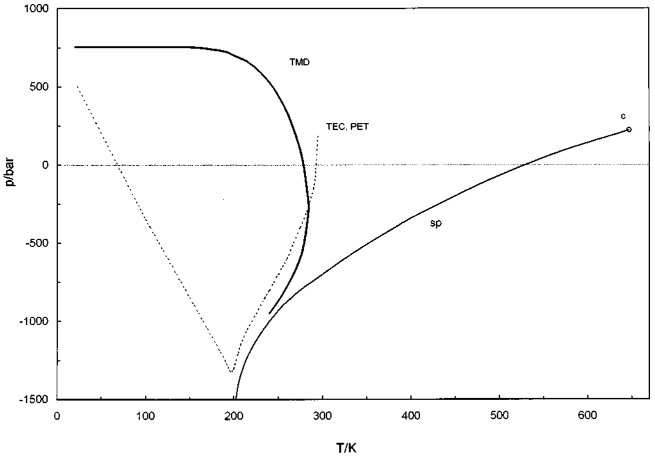

FIG. 2. Model predictions with $\epsilon(=5.353\times 10^3\ \mathrm{J\,mol^{-1}})$ and $v_0(=4.721\times 10^{-5}\ \mathrm{m^3\,mol^{-1}})$ fitted to water's critical temperature and pressure; and $\delta b/b=1.5$, $J/\epsilon=0.5$, $q=100$, $\gamma=4$. The line labeled TEC, PET is the locus of temperatures of compressibility extrema (or, equivalently, pressures of extrema of the thermal expansion coefficient).

ity extrema (maxima at low temperature; minima at high temperature), but only a single thermal expansion extremum.

Figure 1(b), which must be ''read'' along isotherms, shows the corresponding pressure extrema. As demanded by thermodynamic consistency [Eq. (3)], the locus of temperature extrema of K_T coincides with that of pressure extrema of α_p. As in Fig. 1(a), minima are denoted by thin lines, and maxima by thick ones. Note, once again, the proximity of the low-temperature extrema loci. These correspond to temperature-dependent pressures along which the response functions exhibit maxima upon decompression. In the case of α_p, which is negative at temperatures lower than the TMD at any given pressure, this extremum is a locus of maxima in the absolute value of the thermal expansion coefficient.

Figure 2 shows the superheated liquid spinodal, TMD, and the locus of temperatures of compressibility extrema (TEC) (or, equivalently, pressures of extrema of the thermal expansion coefficient, PET). Actual pressures and temperatures were obtained by fitting ϵ and ν_0 to match the critical temperature and pressure of water (647.1 K and 220.55 bar). The calculated temperature along the TMD at 1 bar, 278.75 K, is very close to the actual value for water,[28,29] 277.13 K. According to this choice of parameters, the ''nose'' of the TMD occurs at -271 bar and 283.7 K, and the slope of the TMD at 1 bar is $-27.03\ \mathrm{bar\,K^{-1}}$. The experimental value for the latter quantity[28,29] is $-50\ \mathrm{bar\,K^{-1}}$.

In Figs. 1 and 2 the loci of response function extrema and the TMD meet at a common limiting high-pressure point along the pressure axis (e.g., $P\nu_0/\epsilon\approx 0.5$, $T=0$ in Fig. 1). This limiting behavior of the TMD occurs at fractional occupancies (n) extremely close to unity. Thus, isothermal compression starting from any state point where $\alpha_p<0$ leads eventually to crossing of the TMD and reversion to positive thermal expansion. The low-pressure behavior of the TMD, on the other hand, is different. Within the range of parameters studied, the TMD closely parallels, but does not intersect, the superheated liquid spinodal under tension, as shown in Figs. 1 and 2.

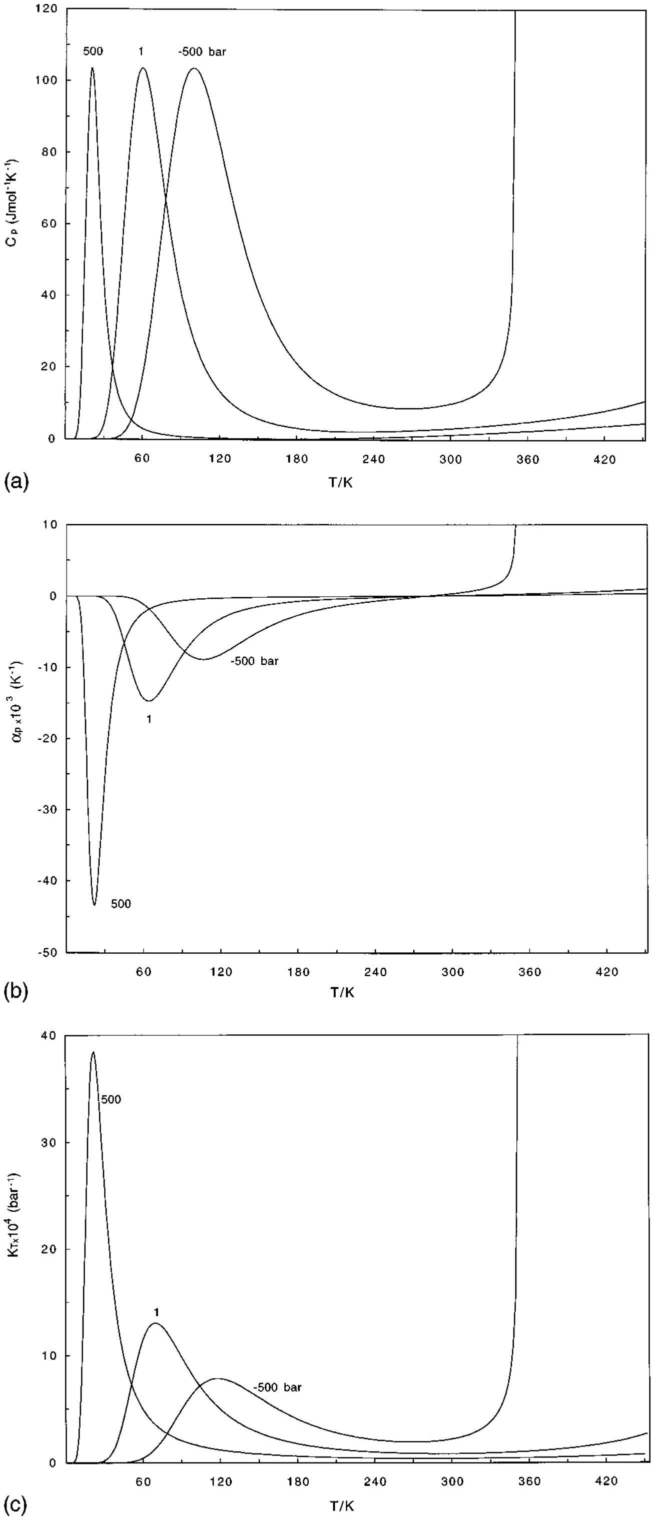

FIG. 3. Temperature dependence of the isobaric heat capacity (a), thermal expansion coefficient (b), and isothermal compressibility (c) at three different pressures. Model parameters as in Fig. 2.

Figures 3(a)–3(c) show the calculated temperature dependence of the three response functions upon isobaric supercooling, at three different pressures. The increase along the -500 bar line at higher temperatures occurs as the superheated liquid spinodal is approached. The three response functions increase sharply upon isobaric cooling. The isothermal compressibility and the isobaric heat capacity exhibit

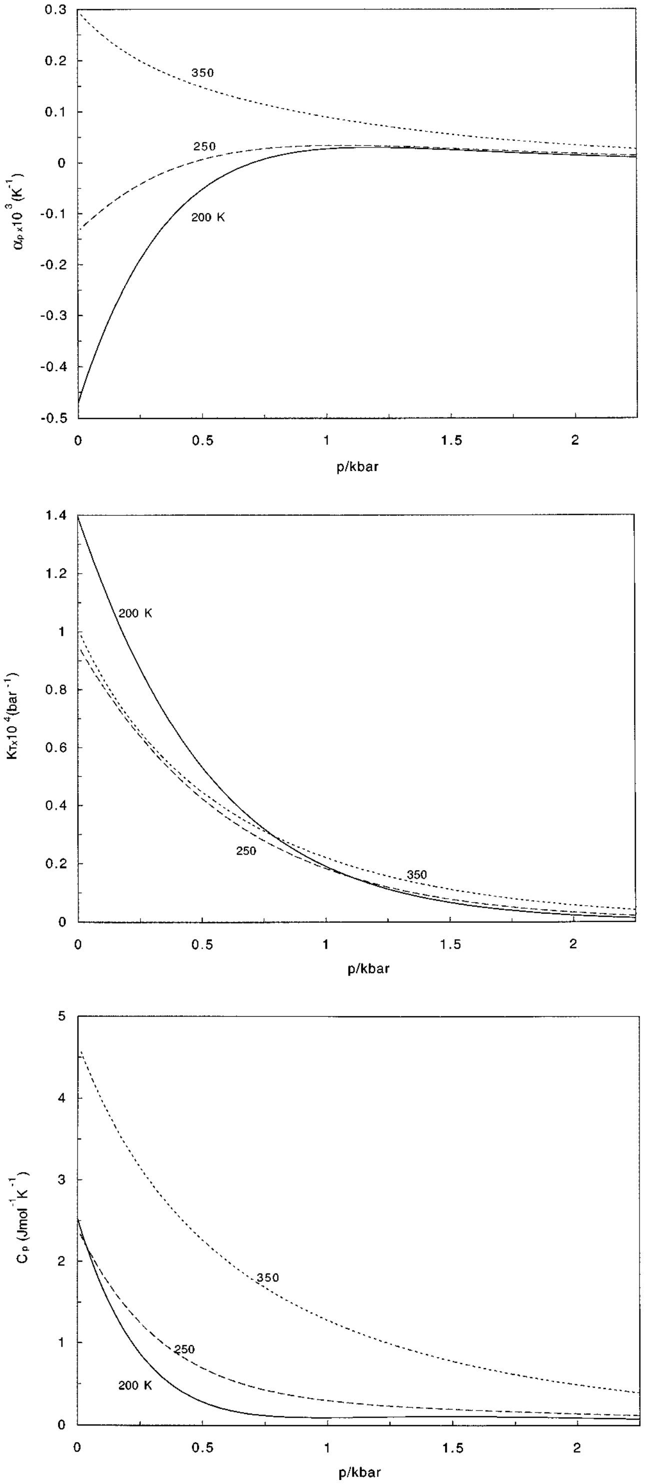

FIG. 4. Detail of the pressure dependence of the thermal expansion coefficient (a), isothermal compressibility (b), and isobaric heat capacity (c) at three different temperatures. Model parameters as in Fig. 2.

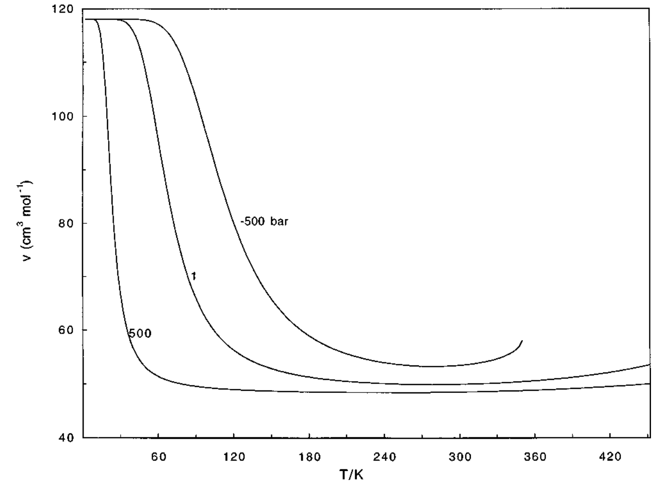

FIG. 5. Low-temperature behavior of the molar volume along three different isobars. Note the pronounced increase in volume upon cooling, which becomes sharper the lower the temperature and the higher the pressure. Model parameters as in Fig. 2.

minima at higher temperatures, but the thermal expansion coefficient shows only the low-temperature extremum. At the experimentally accessible temperatures[5] (e.g., >228 K at 1 bar), the three response functions decrease sharply in magnitude upon isothermal compression. All of these trends are in accord with experimental observations.[1] The minima in the isothermal compressibility and isobaric heat capacity at 1 bar occur at 293.8 and 229.5 K, respectively; the corresponding experimental values[29,30] are 319 and 311 K. The distinguishing feature of Fig. 3 is the fact that the increase in the response functions upon cooling is finite. There are, in other words, no low-temperature singularities. This is in accord with the small-angle x-ray scattering measurements of the structure factor of supercooled water by Xie *et al.*,[23] and with the theoretical predictions of Stanley and Teixeira.[17] An interesting prediction of the model is the relative constancy of the value of the heat capacity maxima, in contrast with the other two response functions, the extrema values of which show a marked increase in absolute value as the pressure is increased.

Figure 4 shows, in detail, the isothermal pressure dependence of the response functions. In accord with experiment, both the compressibility[31] and the heat capacity are suppressed by the application of pressure. In contrast, the thermal expansion coefficient increases upon pressurization at low temperature (i.e., it becomes less negative, and, eventually, positive), and decreases upon pressurization at high enough temperatures. This is also in accord with experimental observations.[30,32]

The corresponding behavior of the volume and the entropy at low temperatures is shown in Figs. 5 and 6, respectively. Consistent with the sharp increases in the isothermal compressibility and the isobaric heat capacity, the model predicts that water will undergo a sharp increase in specific volume and a corresponding decrease in entropy upon isobaric cooling. The higher the pressure, the more abrupt the change in volume and entropy, and the lower the temperature at which this sudden change occurs. Experimentally, this type of behavior would be very difficult to distinguish from a true first-order phase transition between glassy phases[19] with a negatively sloped coexistence locus in the (P,T) plane. Thus, in the singularity-free scenario, there is no phase transition between different forms of liquid (or glassy) water, as has been proposed to exist.[9–16] Rather, at low enough temperatures and high enough pressures, water is predicted to undergo an abrupt but continuous change toward a condition

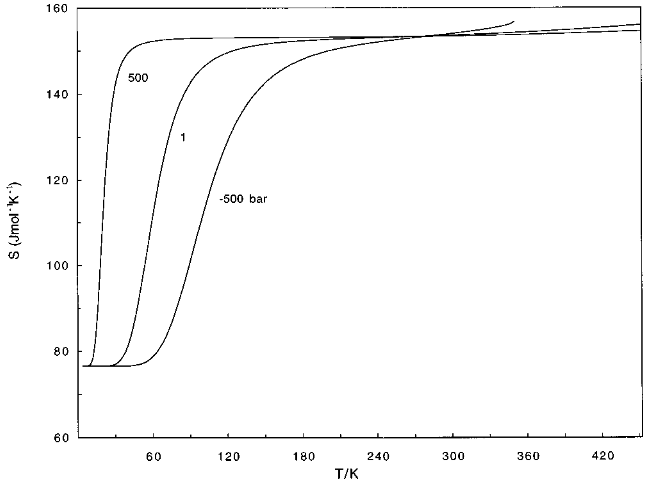

FIG. 6. Low-temperature behavior of the molar entropy along three different isobars. Note the pronounced decrease in entropy upon cooling, which becomes sharper the lower the temperature and the higher the pressure. Model parameters as in Fig. 2.

of low entropy and density. The inflection points in the isobars define a line in the (P,T) plane in the immediate vicinity of which this transition occurs.

The model treats each bond that a molecule can form independently; therefore, there is a low-temperature residual entropy of $\gamma/2 \ln q$ associated with the absence of orientational correlations between bonds, as shown in Fig. 6.

V. CONCLUSION

In this paper we have investigated the singularity-free interpretation of the thermodynamics of supercooled water.[17,18] We have used an idealized compressible lattice model that displays complex waterlike features.[18] In particular, the model exhibits a negative thermal expansion coefficient over a broad region of the phase diagram, and a retracing locus of density maxima.[9,18] Furthermore, the model displays the simplest thermodynamically consistent behavior that is in accord with experimental measurements of anomalies in the response functions of supercooled water. The interpretation that we have studied in detail here explains the anomalous increases in compressibility, heat capacity, and thermal expansion coefficient without invoking an underlying singularity.[17,18] An interesting and complementary singularity-free interpretation of supercooled water at low temperatures that is based on dynamics, rather than thermodynamics, has been proposed recently by Sciortino and co-workers.[33–35] In contrast to the singularity-free picture, the two other interpretations of the thermodynamics of supercooled water explain the experimental observations by postulating the existence of a line of first-order phase transitions[9–16] or a retracing spinodal curve.[6–8]

The salient feature of the singularity-free scenario is the appearance of sharp but continuous changes in density and entropy at low temperatures. As the liquid is supercooled isobarically, the singularity-free scenario predicts that both density and entropy will decrease suddenly though continuously. The abruptness of these changes becomes more pronounced the lower the temperature and the higher the pressure. The main point that we wish to make in connection with experiments is that such abrupt changes in density and entropy as are shown in Figs. 5 and 6 may be very difficult to distinguish experimentally from a true first-order transition,[19] because at the very low temperatures involved noncrystalline water is a glass.[36] Thus, an unambiguous resolution of the question whether water has a second critical point[16] may require experiments specifically designed to probe critical phenomena, rather than simply changes in enthalpy or entropy.[19,21,22] The important recent work of Mishima and Stanley[37] on the decompression-induced melting of ice IV and its relation to a phase transition between two distinct forms of amorphous water illustrate the difficulty of proving (or disproving) experimentally the coexistence between glassy phases.[38]

ACKNOWLEDGMENTS

P.G.D. gratefully acknowledges the support of the Department of Energy, Division of Chemical Sciences, Office of Basic Energy Sciences (Grant No. DE-FG02-87ER13714), and of the donors of the Petroleum Research Fund, Administered by the American Chemical Society.

[1] P. G. Debenedetti, *Metastable Liquids. Concepts and Principles* (Princeton University Press, Princeton, NJ, 1996).
[2] C. A. Angell, in *Water—A Comprehensive Treatise*, edited by F. Franks, (Plenum, New York, 1982), Vol. 7, Chap. 1.
[3] C. A. Angell, Annu. Rev. Phys. Chem. **34**, 593 (1983).
[4] C. A. Angell, J. Shuppert, and J. C. Tucker, J. Phys. Chem. **77**, 3092 (1973).
[5] R. J. Speedy and C. A. Angell, J. Chem. Phys. **65**, 851 (1976).
[6] R. J. Speedy, J. Phys. Chem. **86**, 982 (1982).
[7] M. C. D'Antonio and P. G. Debenedetti, J. Chem. Phys. **86**, 2229 (1987).
[8] P. G. Debenedetti and M. C. D'Antonio, AIChE. J. **34**, 447 (1988).
[9] P. H. Poole, F. Sciortino, U. Essman, and H. E. Stanley, Nature (London) **360**, 324 (1992).
[10] P. H. Poole, F. Sciortino, U. Essman, and H. E. Stanley, Phys. Rev. E **48**, 3799 (1993).
[11] H. Tanaka, Nature (London) **380**, 328 (1996).
[12] P. H. Poole, F. Sciortino, T. Grande, H. E. Stanley, and C. A. Angell, Phys. Rev. Lett. **73**, 1632 (1994).
[13] C. J. Roberts and P. G. Debenedetti, J. Chem. Phys. **105**, 658 (1996).
[14] C. J. Roberts, A. Z. Panagiotopoulos, and P. G. Debenedetti, Phys. Rev. Lett. **77**, 4386 (1996).
[15] S. Harrington, R. Zhang, P. H. Poole, F. Sciortino, and H. E. Stanley, Phys. Rev. Lett. **78**, 2409 (1997).
[16] H. E. Stanley, L. Cruz, S. T. Harrington, P. H. Poole, S. Sastry, F. Sciortino, F. W. Starr, and R. Zhang, Physica A **236**, 19 (1997).
[17] H. E. Stanley and J. Teixeira, J. Chem. Phys. **73**, 3404 (1980).
[18] S. Sastry, P. G. Debenedetti, F. Sciortino, and H. E. Stanley, Phys. Rev. E **53**, 6144 (1996).
[19] O. Mishima, J. Chem. Phys. **100**, 5910 (1994).
[20] O. Mishima, Nature (London) **384**, 546 (1996).
[21] Y. P. Handa, O. Mishima, and E. Whalley, J. Chem. Phys. **84**, 2766 (1986).
[22] M. A. Floriano, Y. P. Handa, D. D. Klug, and E. Whalley, J. Chem. Phys. **91**, 787 (1989).
[23] Y. Xie, K. F. Ludwig Jr., G. Morales, D. E. Hare, and C. M. Sorensen, Phys. Rev. Lett. **71**, 2050 (1993).
[24] D. Eisenberg and W. Kauzmann, *The Structure and Properties of Water* (Oxford University Press, New York, 1969).
[25] J. S. Rowlinson and F. L. Swinton, *Liquids and Liquid Mixtures*, 3rd ed. (Butterworths, London, 1982).
[26] C. A. Angell, M. Oguni, and W. J. Sichina, J. Phys. Chem. **86**, 998 (1982).
[27] D. E. Hare and C. M. Sorensen, J. Chem. Phys. **84**, 5085 (1986).
[28] G. S. Kell, J. Chem. Eng. Data **20**, 97 (1975).

[29] *Water—A Comprehensive Treatise*, edited by F. Franks (Plenum, New York, 1972), Vol. 1, Chap. 10.
[30] W. Kauzmann, Coll. Int. CNRS **246**, 63 (1976).
[31] H. Kanno and C. A. Angell, J. Chem. Phys. **70**, 4008 (1979).
[32] H. S. Frank, Science **169**, 635 (1970).
[33] P. Gallo, F. Sciortino, P. Tartaglia, and S.-H. Chen, Phys. Rev. Lett. **76**, 2730 (1996).
[34] F. Sciortino, P. Gallo, P. Tartaglia, and S.-H. Chen, Phys. Rev. E **54**, 6331 (1996).
[35] F. Sciortino, L. Fabbian, S.-H. Chen, and P. Tartaglia, Phys. Rev. E **56**, 5397 (1997).
[36] P. Brüggeller and E. Mayer, Nature (London) **288**, 569 (1980).
[37] O. Mishima and H. E. Stanley, Nature (London) **392**, 164 (1998).
[38] P. G. Debenedetti, Nature (London) **392**, 127 (1998).